Review article

HYDRAULIC FRACTURING AND MICROSEISMICITY: GLOBAL PERSPECTIVE IN OIL EXPLORATION

J.R. Kayal
Mining Geological & Metallurgical Institute of India, Kolkata, India
E-mail: jr.kayal@gmail.com

Abstract. Induced microseismicity is a common phenomenon in oil and gas reservoirs due to changes in internal stress accompanied by hydraulic fracturing and oil-gas extraction. These microseismicity can be monitored to understand the direction and type of hydraulic fracturing and pre-existing faults by precise hypocenter location and focal mechanism studies. Normal as well as strike-slip faulting earthquakes occur due to opening up of new cracks/fractures, and thrust/reverse faulting earthquakes due to compaction or closing of existing fractures.

Further, frequency-magnitude relation (b-value) and fractal dimension (D-value) of the spatial and temporal clusterization of induced microseismicity may be much useful to characterize the fractures/existing faults and the stress regimes. Seismic tomography, on the other hand, can image the heterogeneous velocity structures/perturbations in the reservoir due to fractures and oil-gas-water contents. A few global case studies are illustrated to understand these processes and to draw attention towards importance of these studies in oil industries.

Keywords: Hydraulic Fracturing, Microseismicity, Oil Exploration
DOI: https://doi.org/10.18599/grs.19.3.12

For citation: Kayal J.R. Hydraulic Fracturing and Microseismicity: Global Perspective in Oil Exploration. *Georesursy = Georesources*. 2017. V. 19. No. 3. Part 1. Pp. 222-228. DOI: https://doi.org/10.18599/grs.19.3.12

1.Introduction

Hydraulic fracturing is a process in which liquids, gas or solids (proppants) are pumped or injected into a formation under high pressure to cause cracks in the formation for enhanced oil and gas production. This technique is routinely used to increase permeability in the reservoirs. During or soon after hydraulic fracturing by injection, there will be an increase fluid pressure along existing fault planes as well as along new fracture planes that cause induced microseismicity. The microseismicity from fluid injection at depth associated with hydraulic fracturing have been recorded with reported magnitudes in the range of -3.0 to < 3.0 (e.g. Verdon et al., 2010; Cipolla et al., 2012; Holland, 2013). Sometimes in a seismically active area such process may trigger larger or felt earthquakes ($M \geq 3.0$). Monitoring of microseismicity to understand the fracture growth and fault reactivation may be done using downhole geophones and or by massive surface arrays comprising hundreds of seismometers (e.g. Grechka, 2010; Gei et al., 2011). Clusters of microseismic events are recorded; the short bursts of events can be temporal as well as spatial. The opening of new fractures may generate normal and strike-slip faulting earthquakes and closing of old fractures may cause thrust/reverse faulting earthquakes. Frequency-magnitude relation *(b-value)* as well as fractal dimension (*D-value*) of induced microseismicity may also show variation with time and space, and shed light on seismic characteristics.

Evaluation of spatio-temporal dynamics of induced microseismicity helps to estimate physical characteristics of hydraulic fractures, like its length, propagation and contraction, its direction and penetration, permeability of the reservoir rock etc. (e.g. Shapiro and Dinske, 2007). The hydraulic fractures may grow from 3 m to 20 m, sometimes more, and could be conjugate to preexisting faults. Thus, understanding and monitoring of fluid-induced microseismicity helps to characterize oil and gas reservoirs and the growth of hydraulic fracturing and or reactivation of preexisting fault system.

Applications of microseismic monitoring in oil and gas industry have seen remarkable growth during the past decades (e.g. Maxwell, 2010). Oil and gas companies have made significant expenditures for microseismic monitoring, but face extraordinary technological challenges to fully utilize the results. The efforts are hampered by a number of factors, including an incomplete understanding of seismological processes that are associated with the induced microseismicity. This paper illustrates a few global case studies to understand some aspects of seismological processes of hydraulic fracturing microseismicity in oil and gas boreholes emphasizing its vital applications in oil industry.

2. Microseismicity Monitoring and Analysis

2.1 Monitoring microseismicity and hypocentre locations

The hydraulic fracturing (here after called *hydrofracturing*) microseismicity usually occurs as clusters, and varies with time and space. Monitoring or recording the hydrofracturing microseismicity by *borehole geophones* at depths, the usual practice, may produce good seismograms with higher signal to noise ratio (S/N), but azimuthal control for precise hypocentre locations of the events could be poor. Surface monitoring by hundreds or sometimes thousands of seismometers may produce much precise locations of the microseismic events. The surface seismometers, however, may be installed at a shallower (5~10 m) depth for recording at a higher S/N.

Sometimes even a 50-staion array on the surface in a smaller area can produce better results (e.g. Li et al., 2011, Tselentis et al., 2011). Long period waveforms of the microseismic events due to hydrofacturing give clear P and S arrivals. The long period character is due to the source effect, not the path effect (Bame and Fehler, 1986). The injection into a reservoir creates new fractures, as well as close, shear or open existing fractures. These various failure mechanisms lead to microseismic events which need to be understood in terms of reservoir productivity.

High precision hypocentre locations are extremely necessary to track the direction of fractures/fault structures or changes in the rock masses. Routine or initial locations may be obtained using most widely used Seisan program, which is basically based on multiple regression analysis using an assumed local homogeneous velocity model or an inverted 1D velocity model. However, due to heterogeneities in velocity structure in the reservoir area, the earthquake locations will not be much precise.

For much precise locations of the hypocentres, *hypocentre double difference* (HypoDD) *technique* is mostly used (e.g. Waldhauser and Ellsworth, 2000). A simple homogeneous 1D velocity model is justified in this analysis since in this technique relative relocations of the events are precisely computed. The relative relocations are insensitive to inaccuracies in the velocity model. These locations should be used to understand the active faults and hydrofractures in the oil fields.

In further advancement, the new hydrofracture zones and or the existing fault zones may be imaged by *double differential tomography* (TomoDD) method (Zhang and Thurber, 2003). This is basically a *simultaneous inversion* technique; it not only relocates the events with much higher precision developing inverted 3D velocity structure, but also produce the *tomograms or images* at any desired depth levels to visualise the perturbed or hydrofractured rock masses with heterogeneous velocities due to faults/fractures and fluid/gas content.

2.2 Fault plane solution

Fault plane solution or source mechanism is an important aspect to understand the nature of faulting that caused the earthquakes. The stress orientation plays the main role for different types of faulting, like normal faulting, strike slip faulting and thrust or reverse faulting.

There are two different methods to obtain fault plane solutions. The most classical method is the P-wave first-motion plot on equal area projection. With the digital seismograms, moment tensor solutions may also be obtained by waveform inversion, and the solutions may be compared with the respective first-motion solutions. The moment tensor analysis consists of generating synthetic seismograms and matching it with the observed seismic waveform including the P-wave first motion and its amplitude.

2.3 b-value and D-value estimation

Frequency of seismic events is considered to be a log-linear function of magnitude, corresponding to the power law distribution (Gutenberg and Richter, 1954), and it is given as: $Log_{10}N = a - bM$, where N is the cumulative number of earthquakes having magnitude larger than M, **a** is a constant and **b** is the slope of the log-linear relation. In this analysis cumulative number of seismic events are plotted against magnitude; slope of the log-linear relation is known as *b-value,* which is normally 1.0 in a tectonically active region. This is an important seismological parameter to know stress condition of rock masses.

It has been reported that before a large event, the b-value decreases corresponding to sudden increase of stress in the rock masses. In case of cluster of events due to earthquake swarm, volcanic activity or induced microseismicity, the b-vale may be more (1.5-2.5) (Kayal, 2008).

Fractal dimensions (D), fractal properties of seismicity, a stochastic self-similar structure in time and space distribution of earthquakes, can be measured, which is introduced as a statistical tool to quantify dimensional distribution of seismicity, its randomness and clusterisation (e.g. Hirata, 1989). The fractal dimension of hypocentre distribution of seismicity may be estimated from the correlation integral given by Grassberger and Procaccia (1983): $C_r \sim r^D$, where (C_r) is the correlation function.

The correlation function measures the spacing (r) or clustering of a set of points, which in this case are earthquake hypocentres, and D is fractal dimension. By plotting C(r) against r on a double logarithmic

coordinate, we can obtain the fractal dimension D from the slope of the curve.

Grob and Van der Baan (2011) illustrated that possible values of fractal dimension range between 0 and 3, which indicates the dimension of the embedding space. Interpretation of such limit values is that a set with D = 0 indicates a point i.e., all events clustered into one point; D = 1, a straight line i.e., events are homogeneously along a straight line, D = 2, a planer i.e., the events are homogeneously distributed over a two-dimensional embedding space, and D = 3, a sphere or cube, in a three dimensional space.

3. Case Studies

3.1 Oman Oil Filed

A surface-station network in the Oman oil field was established in 1999 by the Petroleum Development Oman (PDO), one of the pioneer oil industries to monitor hydrofacture microseismicity. In addition to surface-station network, the borehole geophones were also in operation for comparative study. During the period from 1999 to 2007, over 1500 induced microearthquakes were recorded and precisely located by Li et al. (2011) using the double difference seismic tomography (TomoDD); the epicenters and depth sections of the events are shown in Figure 1.

Most of the earthquakes occurred just above the oil layer, which is located at ~ 1.5 km below the surface. The oil and gas reservoir, a deep seated large anticline dome, ~ 15×20 km in size, is dominated by two fault systems with two preferred directions, southeast-northwest and northeast-southwest. The microseismicity trend shows that the northeast-southwest trending major fault system and the conjugate hydrofractures produce the microearthquakes, and these faults/fractures connects the oil horizons in the field (Fig. 1).

Fault plane solutions of some 40 selected events obtained by waveform inversion show normal, strike slip and reverse faulting (Li et al., 2011) (Fig. 1). Most of the events show normal faulting mechanism, some strike-slip and some reverse faulting. The normal or strike-slip faulting earthquakes indicate opening up of new fractures, and the thrust/reverse faulting earthquakes, on the other hand, indicate closing of old fracture zones. The epicentre trend and the determined fault planes indicate reactivation of the preexisting northeast-southwest fault system as well as the conjugate fractures caused the induced microseismicity.

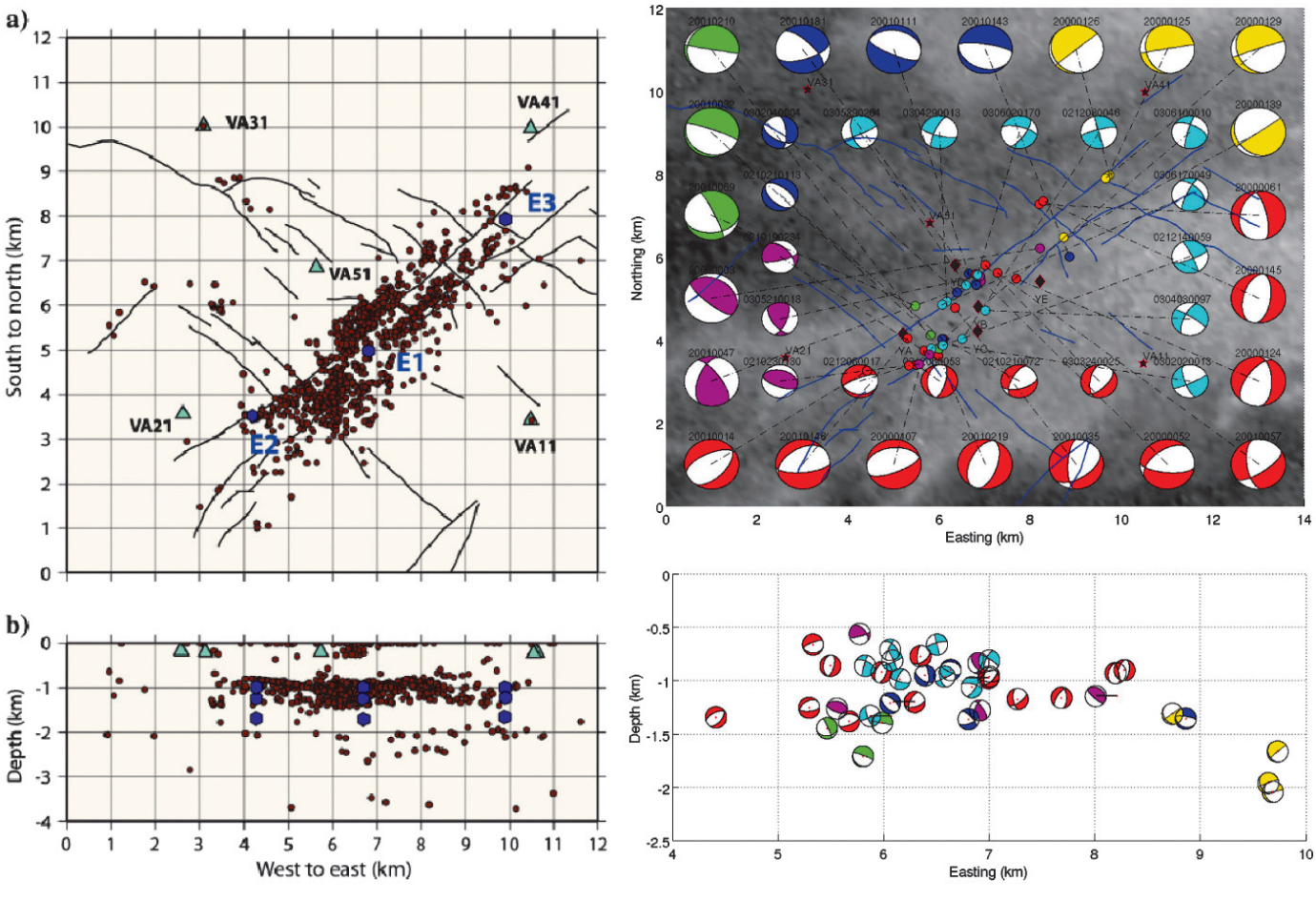

Fig. 1. (a) Left panel shows the precise epicentre map and the right panel shows 40 selected fault plane solutions; shade indicates the topography variation, and (b) left panel shows depth section of the microearthquakes and right panel the fault plane solutions at depths, the Oman oil field (after Li et al., 2011)

It was also found that the maximum horizontal stress derived from the source mechanisms trends in the northeast or north-northeast direction, which is consistent with the direction of the maximum horizontal stress obtained from the well breakout measurements and consistent with the known local tectonic stress (Li et al., 2011).

3.2 Kentucky Oil Field, USA

One of the early studies to map orientation of productive reservoir fractures was conducted in the Clinton County, Kentucky oil field using borehole sensors (Maxwell et al., 2010). In this field, oil is produced from low-porosity carbonate rocks at depths between 300 and 730 m. The existence of isolated fractures with high permeability and storage capacity was evident, but the fracture orientations were unknown and were assumed to be vertical.

The microseismicity monitoring was made near the high-volume production wells. The microearthquke locations and source mechanisms delineate a set of low-angle thrust faults that lie above and below the currently drained interval (Fig. 2). The identification and correlation of these faults with oil production indicated for the first time that these low-angle features should be considered important drilling targets in the exploration and development of the area.

3.3 Alberta Oil Field, Canada

In this case study, we discuss b-value and D-value variation in microseismicity in an oil field in Alberta, Canada. The heavy-oil reservoir is drained using cyclic steam stimulation that produced some 2132 events in seven months, from September 2009 to March 2010. Prior to December 2009, only injection and then a combined injection and production strategy were adopted.

The frequency-magnitude distribution show that the b-value is 1.20 over the reliable magnitude-distribution part of the data set (Fig. 3a). The correlation integral plot estimates a D-value 2.36 over the linear part of the curve (Fig. 3b); this implies that the events are distributed rather spherically in space.

The Figure 3c represents temporal variations of the *b*-value from September 2009 to March 2010. The *b*-values are computed over 300 events with a moving window shift of 30 events. Three different stages are observed as highlighted by the ellipses. At the first stage during steam injection, fracturing with predominant tensional stress causes higher b-value, in the second stage injection and production cause lower b-value, and in the third stage when injection stopped, lowest b-value indicates fracture closing with predominant compression. Similarly, the Figure 3d represents three stages of D-value; the lowest D-values occur in the middle or second stage, indicating the possible presence of strike-slip faulting.

The measured temporal variations in *b-value and D-value show* a strong variation in local stress over a seven-month period; it ranges from extensional faulting (fractures opening), via a strike-slip regime, to finally compressive faulting (fractures closing).

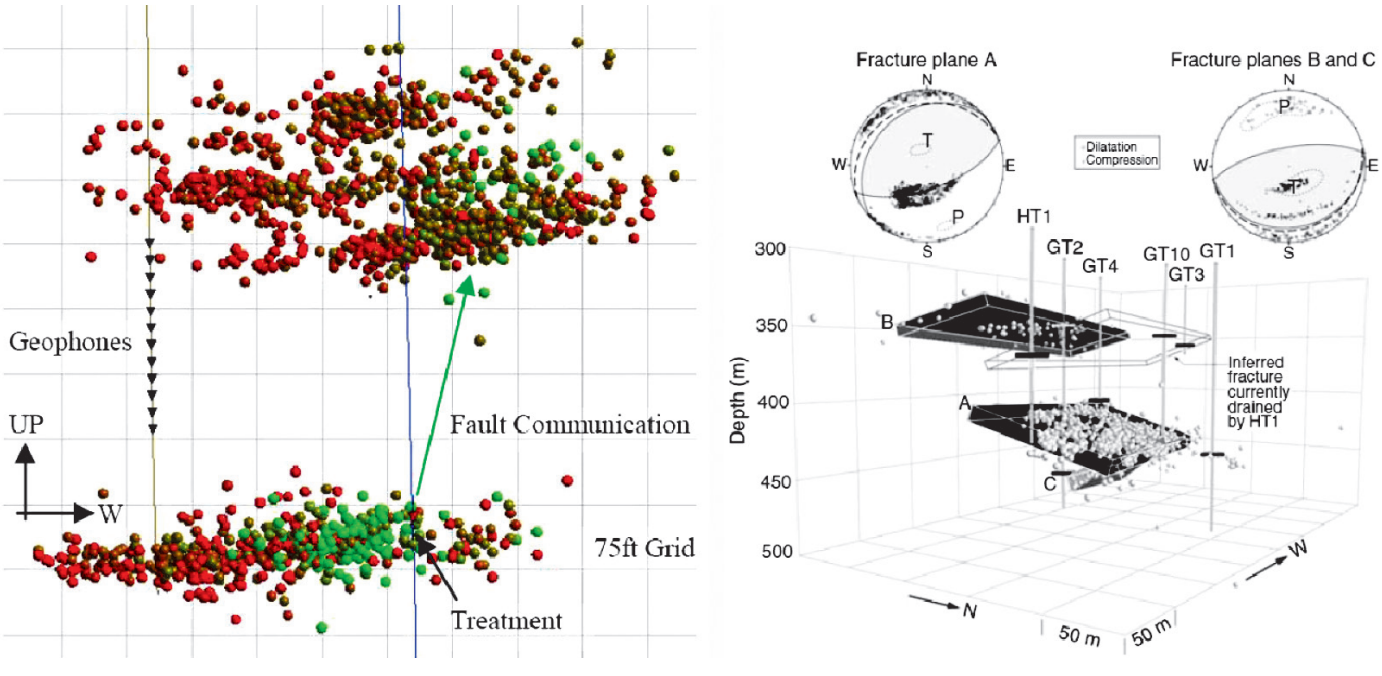

Fig. 2. (a) Depth section of microearthquakes recorded in two formations, the brittle failure occurs first in the right-most part of the bottom formation, and then suddenly jumps to the top sand formation, no activity in the middle shale layer. Green dots indicate microearthquakes when injection started, and red dots when along with injection, production made. (b) Fracture planes defined by 3D plot, the composite fault plane solutions indicate reverse / thrust faulting, Clinton County, Kentucky oil field (after Maxwell et al., 2010)

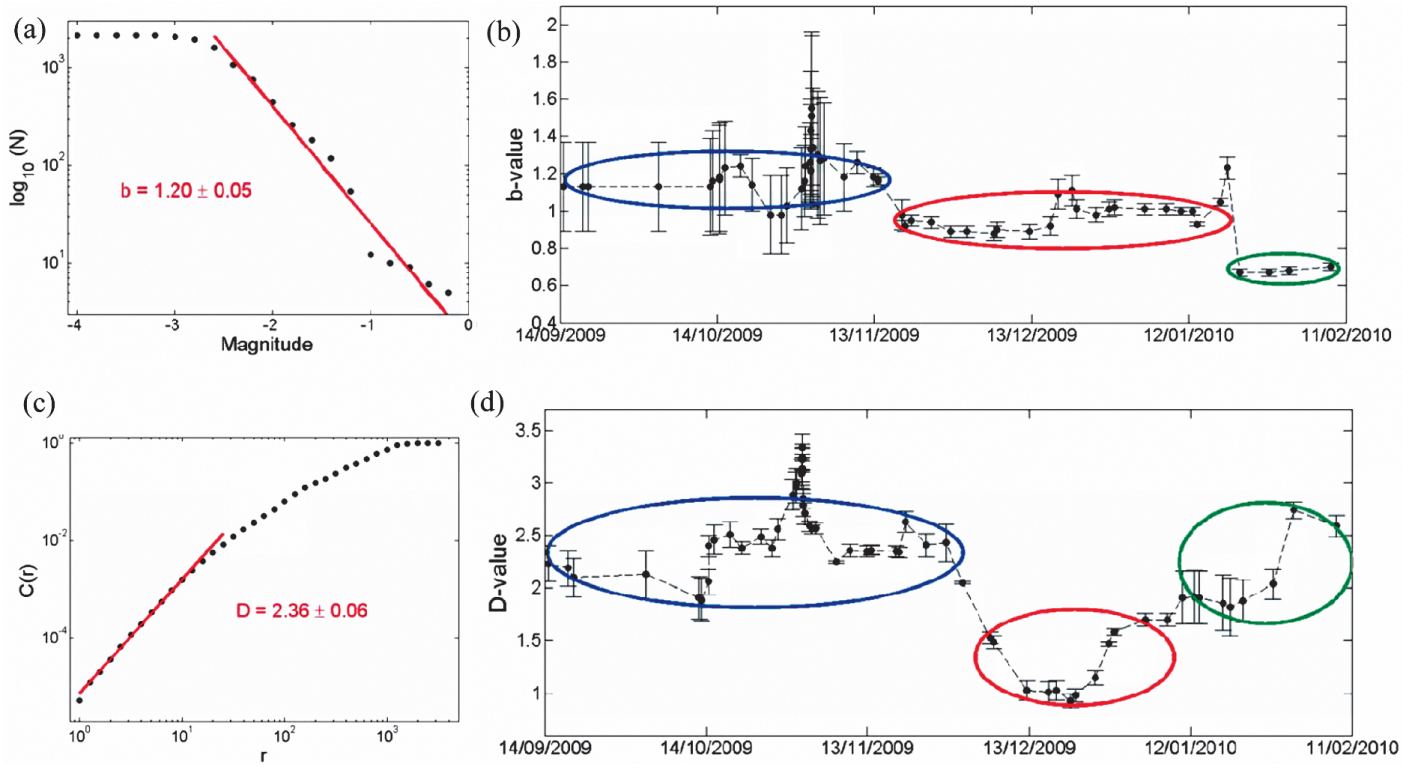

Fig. 3. (a) Frequency-magnitude relation with an average b-value 1.20, (b) temporal evolution of b-values, (c) correlation integral with an average D-value 2.36 and (d) temporal evolution of D-values; the ellipses emphasize the three different stages (see text); heavy-oil data set, Alberta (after Grob and Van der Baan, 2011)

The fractal dimension *D* indicates predominantly planar-to-spherical hypocenter distributions in the first and last stages, but changes to a more linear-to-planar spatial pattern in the middle stage of strike-slip regime.

Thus the microseismic event locations and their magnitudes contain a wealth of information to facilitate reservoir management.

3.4 Delvina hydrocarbon field, Southern Albania, Europe

Here, we discuss the important role of seismic tomography in oil exploration. The Delvina hydrocarbon field was designed with a network of 50 three-component borehole seismometers and 50 three-component surface seismometers. Magnitudes of the events ranged from 0 to 3 with most events occurring between M 1.0-2.0, and hypocentral depths between 0 and 20 km, with most located at depths 2-10 km (Fig. 4). Some 1860 microearthquakes were used in seismic tomography that imaged heterogeneous structures of the oil and gas reservoirs. Some 47,280 phase data, 24,438 P-arrivals and 22,842 S-arrivals, are used for the tomographic simultaneous inversion (Tselentis et al., 2011).

The results provided a wealth of information where conventional 2D seismic surveys did not work well. Using the tomography results two sub-regions of the investigated area are identified, one corresponding to an oil field and the other to a gas field. At the depth (~2 km) where the oil reservoir is encountered, the V_P/V_S values reach a maximum, and it is minimum in the gas field (Fig. 4).

4. Conclusions

This paper made an attempt to emphasize the importance of monitoring hydraulic fracturing microseismicity for better understanding of the fracture growth in oil and gas reservoirs in production. Hydraulic fracture, a rather complex structure, does not allow for modeling with required precision based on reservoir geology and fluid dynamics model.

Precise locations of microseismicity, fault plane solutions, temporal and spatial variations of b-values and D-values and differential seismic tomography can reveal wealth of information for reservoir development and management by mapping anomalous well drainage patterns, defining efficient drilling placement, correcting target depths ahead of the bit during exploratory drilling, correcting interpreted geologic horizon and so on. It is a modern technology in oil industry for efficient management and development.

Acknowledgement

I sincerely thank the Organizing Committee, Daria Khristoforova in particular, for kindly inviting me to

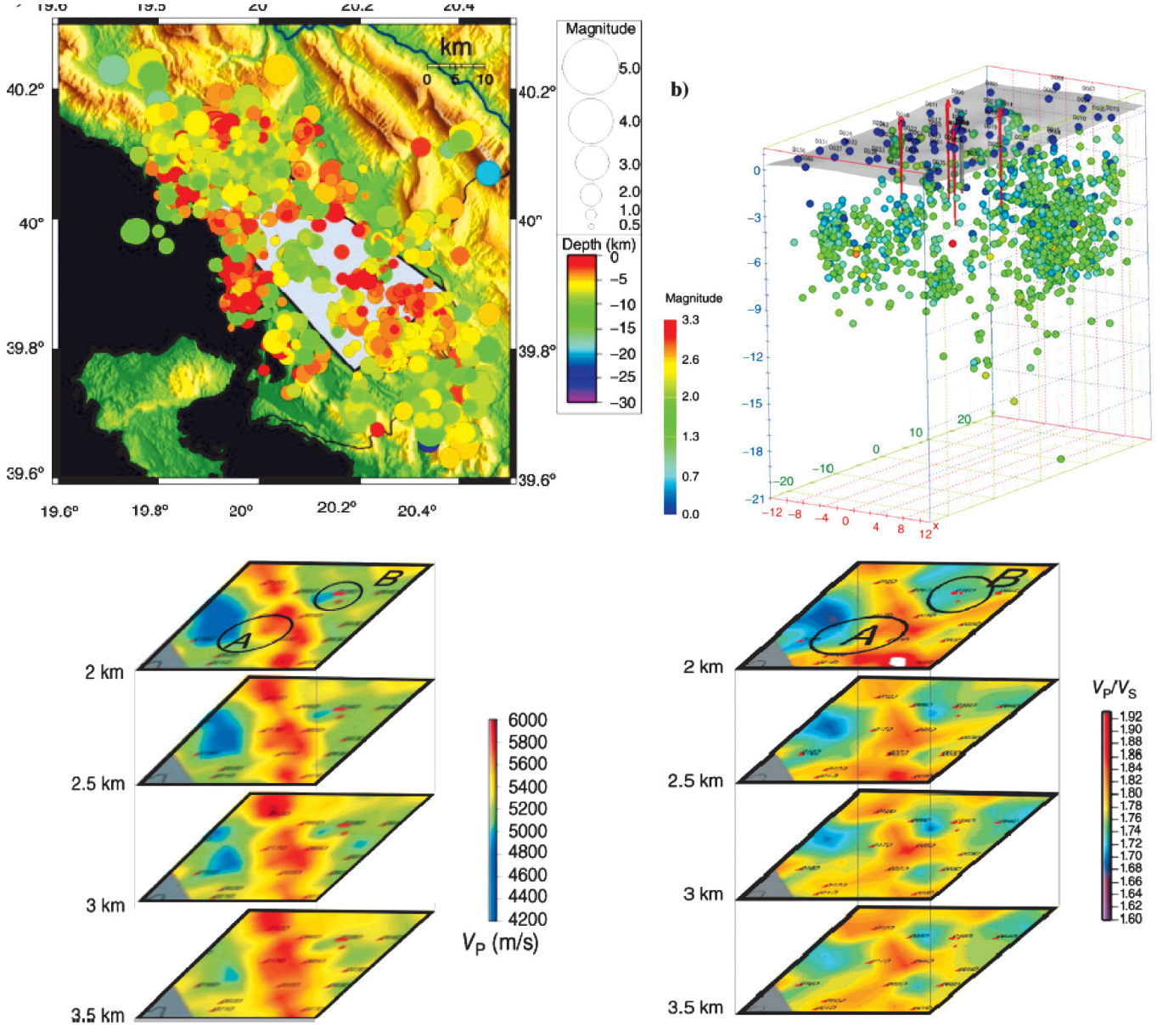

Fig. 4. (a) Microseismicity map, (b) 3D view of the hypocentres, and (c) Seismic Vp and (d) Vp/Vs depth slices differentiating the oil and gas bearing zones, Delvina oil field (after Tselentis et al., 2011)

the important International Scientific and Practical Conference «Horizontal wells and hydraulic fracturing to improve the efficiency of oil fields development» (September 6-7, 2017, Kazan, Russia) to deliver a lecture on such a fascinating topic. Thanks to all Russian friends who extended their kind help and support for giving me this opportunity to enrich myself and to interact with the august gathering in this Conference for future collaboration.

References

Bame, D. and Fehler, M. Conservations of long period earthquakes accompanying hydraulic facturing. *Geophys. Res. Lett*. 1986. 13. 149-152.

Cipolla, C., Maxwell, S., Mack, M. Engineering guide to the application of microseismic interpretations. SPE 152165. 2012.

Gei, D., Eisner, L., Suhadolc, P., Feasibility of estimating vertical transverse isotropy from microseismic data recorded by surface monitoring arrays. *Geophysics*. 2011. 76. WC117- WC126.

Grassberger, P. and Procaccia, I. Characterisation of strange attractors. *Phys. Rev. Lett*. 1983. 50. Pp. 346-349.

Grob, M. and Van der Bann, M. Inferring in-situ stress changes by statistical analysis of microseismic event characteristics. *The Leading Edge*. 2011. Pp. 1296-1301. doi: 142.244.191.132.

Gutenberg, B. and Richter, C. F. Seismicity of the Earth and Associated Phenomena. Princeton University Press, New Jersey. 1954. 310 p.

Hirata, T. A correlation between the b-value and the fractal dimension of earthquakes. *J. Geophys. Res*. 1989. 94. Pp. 7507-7514.

Holland, A. A. Earthquakes Triggered by Hydraulic Fracturing in South-Central Oklahoma. *Bull Seism Soc Am*. 2013. 103. doi: 10.1785/0120120109

Kayal, J. R., 2008. Microearthquake Seismology and Seismotectonics of South Asia. Springer, The Netherlands. 2008. 503 p.

Li, J., Kuleli, S. H., Zhang, H., and Toksöz, M N.Focal mechanism determination of induced microearthquakes in an oil field using full waveforms from shallow and deep seismic networks. Geophysics. 2011. 76(6). doi: 10.1190/GEO2011-0030.1

Maxwell, S. C., Rutledge, J., Jones, R. and Fehler, M. Petroleum reservoir characterization using downhole microseismic monitoring. *Geophysics*. 2010. 75 (5). doi: 10.1190/1.3477966

Maxwell, S. C., Cho, D., Pope, T., Jones, M., Cipolla, C., Mack M., Henery F., Leonard, J. Enhanced reservoir characterisation using hydraulic fracture microseismicity. SPE 140449. 2011.

Shapiro, S.A. and Dinske, C. Fluid-induced seismicity: Pressure diffusion and hydraulic fracturing. *Geophysical Prospecting*. 2009. 57. Pp. 301-310.

Tselentis, G., Martakis, N., Paraskevopoulos, P., and Lois, A. High-resolution passive seismic tomography (PST) for 3D velocity, Poisson's ratio and P-wave quality QP in the Delvina hydrocarbon field, southern Albania, *Geophysics*. 2011. 76(6). doi: 10.1190/1.3560016

Verdon, J. P., J. Michael Kendall, M. and Maxwell, S. C. A comparison of passive seismic monitoring of fracture stimulation from water and CO_2 injection. *Geophysics*. 2010. 75. No. 3. MA1-MA7

Waldhauser, F. and Ellsworth, W.L. A double-difference earthquake algorithm: Method and application to the Northern Hayward Fault, California. *Bull. Seism. Soc. Am*. 2000. 90(6). Pp. 1353-1368.

About the Author

Jnana Ranjan Kayal – Ph D (Seismology), Retd. Deputy Director General (Head, Geophysics), Geological Survey of India; Life member, Mining Geological and Metallurgical Institute

73B Thakurpukur Road, Kolkata 700063, India

Tel: +91-9830675424, e-mail: jr.kayal@gmail.com

Manuscript received 23 June 2017;
Accepted 27 July 2017; Published 30 August 2017